Dynamic hysteretic features of Ising-type thin films

Bahadır Ozan Aktaş
Dokuz Eylül University, Graduate School of Natural and Applied Sciences, TR-35160 Izmir, Turkey

Ümit Akıncı and Hamza Polat*
Department of Physics, Dokuz Eylül University, TR-35160 Izmir, Turkey
(Received 10 May 2014; published 28 July 2014)

In order to elucidate the nature of hysteresis characteristics in a magnetic Ising-type thin film with a certain thickness, such as types of frequency dispersion curves, decay of hysteresis loop area, corresponding coercive field and remanent magnetization values, etc., we investigate the hysteretic response of each layer within effective-field theory. Throughout the analysis, the best appropriate parameter values are chosen since they would allow us to observe the reversed magnetic hysteresis after a certain value of external field frequency. This eccentric phenomenon has prompted us to associate it to the domain nucleation and growth mechanism in the dynamic process. Exotic shapes of the response for different layer indices in two different regimes of modified surface exchange are particularly emphasized.

DOI: 10.1103/PhysRevE.90.012129 PACS number(s): 64.60.Ht, 75.60.−d, 75.70.Kw

I. INTRODUCTION

Hysteresis is the signature of how cooperative many-body system parameters respond dynamically to an alternating external magnetic field sweep. For kinetic Ising-type systems, the most familiar one is in the form of a Lissajous curve and essentially originated from the variation of ordinary (time-dependent) magnetization with an external field. This ubiquitous phenomenon has been the subject of intensive interest due to a broad range of applications. Hysteretic behavior is, however, a complicated process of a dynamic and nonlinear nature that eludes serious treatment, both experimentally and theoretically, since the area enclosed by the hysteresis loop (HL) is directly proportional to the energy loss in a magnetization-demagnetization cycle. In order to understand and clarify the behavior of the system under consideration, the remanent magnetization (in other words residual magnetization, which is the magnetization left behind in the system after the external magnetic field is removed) and coercive field (which means the intensity of the external magnetic field needed to change the sign of the magnetization) has been calculated several times in the literature by benefiting from the hysteresis. An HL areal scaling law, which enables a universality classification, was manifested first by Steinmetz [1] empirically in his pioneering work dating back to the end of the nineteenth century.

Many efforts have been devoted to making a prediction for experimental verification of the hysteresis loop area (HLA) scaling for thin films (for a brief review of HLA scaling results see Ref. [2]). A recent series of studies of usual characteristics of the hysteretic response in thin films have been also presented by different researchers [3–6]. The surface critical properties at a dynamic phase transition have been presented very accurately by Park and Pleimling [7]. According to their findings, the kinetic surface phase diagram in three dimensions is remarkably simple and does not exhibit a special transition point or a surface or extraordinary transition.

Low coercivity, which means low hysteresis loss per cycle of operation, is desired in core materials (or it is used only for temporal magnetic recording). On the other hand, high coercivity is used in applications where the magnetic recording media is frequently used or the long-lifetime recording is needed. This strategy is the main trensetter in magnetic thin film design [8]. Controlling thickness of a film to obtain the magnetic hysteresis at the right shape to suit the desired technological purpose is the key issue in disguise [5]. Therefore, how the spontaneous spin formation mechanism involves these reduced structures becomes the focus of frequent investigation issues. Due to the underlying complexity of the reduced dimension, any systematic investigation regarding the hysteresis behavior and its influences on each layer does not exist. So some important issues remain unresolved: the frequency dispersion of HLA with corresponding remanence and coercivity for different layer indices, classification of dispersion curves, topological evolution of the hysteretic response of each layer while varying the modified surface exchange, etc.

Consequently, the aim of this study is to give a more complete picture of the overall hysteretic behavior of ferromagnetic thin films for different values of modified exchange interaction at a fixed temperature (the temperature has been selected for a certain criterion). For this purpose, we first investigate how the hysteretic properties of a film depend on the dynamic system parameters by means of effective-field theory (EFT) including their relevant dispersion curves. After that, we present a sort of well-selected hysteresis collection (they have been selected precisely from the frequency dispersion of the HLA) to observe how the response depends on the layer index. Finally we discuss the magnetization reversal mechanism within reasonable bounds.

II. METHODOLOGY

From the theoretical point of view, the most widely used model to study the magnetic properties of surfaces is a Ising model due to the crossover of dimensionality and strong uniaxial anisotropy. So the system can be modeled by a layered Ising-type structure which consists of interacting

*hamza.polat@deu.edu.tr

parallel layers. Each layer is defined as a regular lattice with coordination number $z = 4$. The Hamiltonian is given by

$$\mathcal{H} = -\sum_{\langle ij \rangle} J_{ij} s_i s_j - h(t) \sum_i s_i, \tag{1}$$

where s_i is the spin operator on lattice site i and any spin variable can take the values $s_i = \pm 1$. A $\langle \cdots \rangle$ subscript bracket symbolizes the nearest neighboring in the first summation. The second summation is over all the lattice sites. The exchange interaction J_{ij} between the spins on the sites i and j takes the values according to the positions of the nearest neighbor spins. Two surfaces of the film have intralayer coupling J_1. The interlayer coupling between the surface and its adjacent layer (i.e., layers 1, 2, and L, $L-1$) is denoted by J_2. For the rest of the layers, the interlayer and the intralayer couplings are assumed as J_3. The system has three exchange interactions where J_1, J_2, $J_3 > 0$ favor a ferromagnetic alignment of the adjacent sites as shown in Fig. 1 of our prior work (see Ref. [9]). The Zeeman term describes interaction of the spins with the field of the sinusoidal form

$$h(t) = h_0 \cos(\omega t), \tag{2}$$

where t is the time and h_0 is the amplitude of the oscillatory magnetic field with an angular frequency ω.

Our system is in contact with an isothermal heat bath at given temperature T. So the dynamical evolution of the system may be given by nonequilibrium Glauber dynamics [10] based on a master equation. The number of L different magnetization time series for the system can be given by the usual dynamical EFT equations, which are obtained by the differential operator technique [11,12]. In order to handle the multispin correlations, a decoupling approximation (DA) [13] can be used as

$$\left\langle s_i^{(k)} \cdots s_j^{(k)} \cdots s_l^{(k)} \right\rangle = \left\langle s_1^{(k)} \right\rangle \cdots \left\langle s_j^{(k)} \right\rangle \cdots \left\langle s_l^{(k)} \right\rangle, \tag{3}$$

which is essentially identical to the Zernike approximation [14] in the bulk problem, and it has been successfully applied to a great number of magnetic systems including the surface problems [15–17]. Thus, the dynamical equations of motion for each layer are in the form

$$\begin{aligned}
\tau \frac{dm_1}{dt} &= -m_1 + [A_1 + m_1 B_1]^z [A_2 + m_2 B_2], \\
\tau \frac{dm_2}{dt} &= -m_2 + [A_2 + m_1 B_2][A_3 + m_2 B_3]^z [A_3 + m_3 B_3], \\
&\vdots \quad \vdots \qquad\qquad \vdots \\
\tau \frac{dm_k}{dt} &= -m_k + [A_3 + m_{k-1} B_3][A_3 + m_k B_3]^z [A_3 + m_{k+1} B_3], \\
&\vdots \quad \vdots \qquad\qquad \vdots \\
\tau \frac{dm_{L-1}}{dt} &= -m_{L-1} + [A_3 + m_{L-2} B_3][A_3 + m_{L-1} B_3]^z [A_2 + m_L B_2], \\
\tau \frac{dm_L}{dt} &= -m_L + [A_2 + m_{L-1} B_2][A_1 + m_L B_1]^z.
\end{aligned} \tag{4}$$

Here the magnetization time series of kth layer m_k is defined as

$$m_k = \left\langle s_i^{(k)} \right\rangle, \quad k = 1, \ldots, L, \tag{5}$$

with the coefficients

$$\begin{aligned}
A_n &= \cosh(J_n \nabla) f(x)|_{x=0}, \\
B_n &= \sinh(J_n \nabla) f(x)|_{x=0}.
\end{aligned} \tag{6}$$

$n = 1,2,3$ and $\nabla = \partial/\partial x$ is one-dimensional differential operator, and the function $f(x)$ is given by

$$f(x) = \tanh\{\beta[x + h(t)]\}. \tag{7}$$

Here $\beta = 1/k_B T$ and k_B represent the Boltzmann constant. The effect of the differential operator on an arbitrary function $f(x)$ is

$$\exp(a\nabla) f(x)|_{x=0} = f(x + a)|_{x=0}, \tag{8}$$

with any real constant a.

By using the binomial expansion and the hyperbolic trigonometric functions in terms of the exponential functions we get the most compact form of Eq. (4):

$$\begin{aligned}
\dot{m}_1 &= \frac{1}{\tau}\left[-m_1 + \sum_{\gamma=0}^{z} \sum_{\eta=0}^{1} \Lambda_1(\gamma,\eta) m_1^\gamma m_2^\eta \right], \\
\dot{m}_2 &= \frac{1}{\tau}\left[-m_2 + \sum_{\gamma=0}^{z} \sum_{\eta=0}^{1} \sum_{\nu=0}^{1} \Lambda_2(\gamma,\eta,\nu) m_2^\gamma m_1^\eta m_3^\nu \right], \\
&\vdots \quad \vdots \qquad\qquad\qquad \vdots \\
\dot{m}_k &= \frac{1}{\tau}\left[-m_k + \sum_{\gamma=0}^{z} \sum_{\eta=0}^{1} \sum_{\nu=0}^{1} \Lambda_3(\gamma,\eta,\nu) m_k^\gamma m_{k-1}^\eta m_{k+1}^\nu \right], \\
&\vdots \quad \vdots \qquad\qquad\qquad \vdots \\
\dot{m}_{L-1} &= \frac{1}{\tau}\left[-m_{L-1} + \sum_{\gamma=0}^{z} \sum_{\eta=0}^{1} \sum_{\nu=0}^{1} \Lambda_2(\gamma,\eta,\nu) m_L^\gamma m_{L-1}^\eta m_{L+1}^\nu \right], \\
\dot{m}_L &= \frac{1}{\tau}\left[-m_L + \sum_{\gamma=0}^{z} \sum_{\eta=0}^{1} \Lambda_1(\gamma,\eta) m_L^\gamma m_{L-1}^\eta \right],
\end{aligned} \tag{9}$$

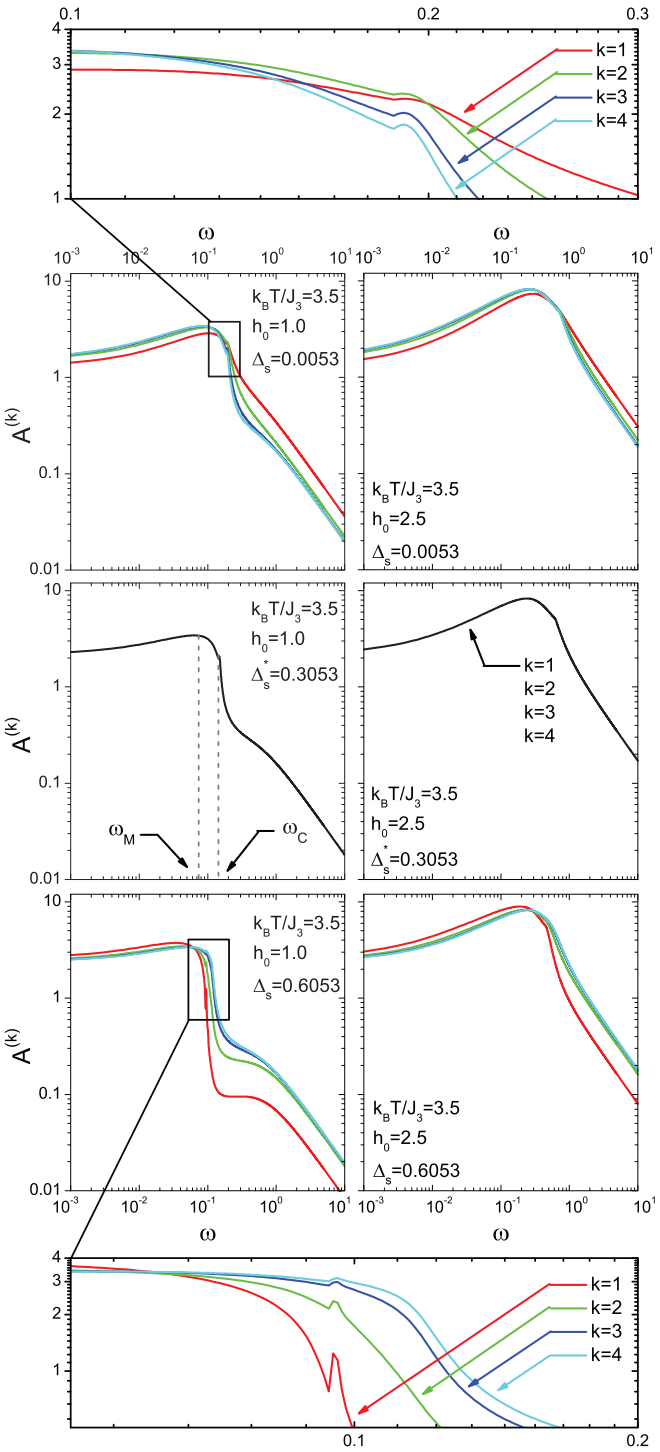

FIG. 1. (Color online) The frequency dispersion of HLA for each layer of $L = 7$ at a fixed temperature $k_B T/J_3 = 3.5$. The curves were plotted for the selected amplitude representatives as $h_0 = 1.0$ and 2.5 in each group of triple columns. The sequence of dispersions is reversed in two different regimes of modified exchange interaction.

where

$$\Lambda_1(\gamma,\eta) = \binom{z}{\gamma}\binom{1}{\eta} A_1^{z-\gamma} A_2^{1-\eta} B_1^{\gamma} B_2^{\eta},$$
$$\Lambda_2(\gamma,\eta,\nu) = \binom{z}{\gamma}\binom{1}{\eta}\binom{1}{\nu} A_2^{1-\eta} A_3^{z+1-\gamma-\nu} B_2^{\eta} B_3^{\gamma+\nu}, \quad (10)$$
$$\Lambda_3(\gamma,\eta,\nu) = \binom{z}{\gamma}\binom{1}{\eta}\binom{1}{\nu} A_3^{z+2-\gamma-\eta-\nu} B_3^{\gamma+\eta+\nu}.$$

Here $1/\tau$ is transition per unit time in a Glauber-type stochastic process, and throughout our calculations we set it as $\tau = 1$ for simplicity. It is clear that solving the set of self-consistent nonlinear ordinary differential equations given in Eq. (9) is essentially an initial value problem. In order to get the $m_k(t)$ time series for each, we use standard fourth-order Runge-Kutta method (RK4).

The system has three dependent Hamiltonian variables: frequency and amplitude of an external magnetic field, respectively, ω, h_0, and the thickness L. For fixed values of these parameters together with temperature and interaction constants J_1, J_2, J_3, RK4 solutions will give convergency behavior after some iterations; i.e., the solutions have the property $m(t) = m(t + 2\pi/\omega)$ for an arbitrary initial value for the magnetization $[m(t = 0)]$. Each iteration, i.e., the calculation of magnetization at the $t + 1$ time step from previous magnetization for t, is now performed for these purposes, whereby the RK4 iterative equation is being utilized to determine the magnetization for every i. In order to keep the iteration procedure stable in our simulations, we have chosen 10^4 points for each RK4 step. Thus, after obtaining the convergent region and some transient steps (which depends on Hamiltonian parameters and the temperature) the dynamical order parameter (DOP) for each layers can be calculated from

$$Q_k = \frac{\omega}{2\pi} \oint m_k(t)\, dt, \quad (11)$$

where m_k is a stable and periodic function.

As a cutoff condition for numerical self-consistency, we defined a tolerance

$$\left| Q_k \right|_{t-2\pi/\omega}^{t} - Q_k \left|_{t}^{t+2\pi/\omega} \right| < 10^{-5}, \quad (12)$$

meaning that the maximum error as the difference between each consecutive iteration should be lower than 10^{-5} for all steps. DOP accurately can be calculated from this stationary solutions of $m_k(t)$ over a cycle. On the other hand, the energy loss due to the hysteresis, in other words, HLA, is defined as

$$A^{(k)} = -\oint m_k(t)\, dh(t) = h_0 \omega \oint m_k(t) \sin(\omega t), \quad (13)$$

and the modified surface exchange interaction has been defined to determine the different characteristic behavior of the system in a certain range as

$$J_1 = J_3(1 + \Delta_s). \quad (14)$$

There are three possible orders of the system: F, P, and the coexistence phase (F+P). In the P phase, $m(t)$ in a convergent region for any layer is satisfied by the condition

$$m(t) = -m(t + \pi/\omega), \quad (15)$$

which is called the symmetric solution. On the other hand, in the F phase, the solution does not satisfy Eq. (15), and this solution is called the nonsymmetric solution, which oscillates around a nonzero magnetization value. The solution in the F phase does not follow the external magnetic field; i.e., the value of Q is different from zero. In these two cases, the observed behavior of magnetization is independent from the choice of initial value of magnetization $m(0)$, whereas the last phase has magnetization solutions symmetric or nonsymmetric depending on the choice of the initial value of magnetization

corresponding to the coexistence region where the F and P phases overlap. The main goal of our detailed investigation is adjunctly manifesting the frequency dispersion of HLA and corresponding coercivity ($H_c^{(k)}$) with remanence ($M_r^{(k)}$) of the layers. Note that more details about our formulation and the reasons for the selection procedure about the related values of system parameters at which the calculations carried out can be found in Ref. [9].

III. RESULTS AND DISCUSSION

With the guidance of the work given in Ref. [9], the frequency dispersion of HLA with corresponding coercivity and remanent magnetization for a pure crystalline ferromagnetic thin film with $L = 7$ layers are presented in Figs. 1–3. We see that the frequency dependency for each characteristic has a crossover at a critical value of modified exchange interaction Δ_s^*. There exists a hierarchical change of the HLA sequence for each layer in two different regimes of Δ_s as shown in Fig. 1. For a fixed h_0, the hysteresis loop of the surface has the lowest area in the $\Delta_s < \Delta_s^*$ regime till the symmetry loss. In the other regime ($\Delta_s > \Delta_s^*$) the hysteresis loop of innermost layer has the lowest area. The layer indices are of no importance in frequency dependency at the critical value of modified exchange interaction. In other words, all layers have the same hysteretic behavior at Δ_s^*. The physical mechanism can be briefly explained as follows: When proceeding from the surface to the center of the film, the hysteresis loop becomes larger at lower ω, but it slightly gets smaller at higher ω values for the fixed value of h_0 in $\Delta_s < \Delta_s^*$ regime. There are relatively more neighboring per magnetic sites, which causes locally larger magnetic interaction in inner layers. So it becomes more difficult to follow the external field for any spin. Hysteresis is more likely to be asymmetric in this regime. Surface spins are embedded in an environment of lower symmetry than that of the inner atoms. The exchange constant between atoms in the surface region may differ from the bulk one. The lower Δ_s regime corresponds to a surface type of magnetic ordering with this aspect. The opposite of the above scenarios can be considered also. From a different point of view, if the Δ_s increases (i.e., we are now in the $\Delta_s > \Delta_s^*$ regime), the hysteresis loop becomes smaller at low ω but slightly gets larger at high ω when proceeding from the surface to the center of the film. This is since for inner layers there are more neighboring but far fewer exchange constant per magnetic sites, which causes relatively smaller magnetic interaction than that of the surface one. Eventually, the free surface cannot break the translational symmetry since the hysteretic and/or magnetic properties of the free surfaces exactly overlap with the bulk one at the critical value of surface exchange Δ_s^*. We can say more generally that the deficiency of the interaction strength per surface spin can be compensated by increasing the modified exchange interaction strength. The coercivity and remanent magnetization presented in Figs. 2 and 3 are also consistent with the aforementioned arguments about the mechanism. The profiles across the film differ qualitatively in two regimes ($\Delta_s < \Delta_s^*$ and $\Delta_s > \Delta_s^*$).

A_k increases at low ω values first, and then it reaches the maximum value in agreement with the well-known behavior in the literature where frequency at the peak ω_M corresponds

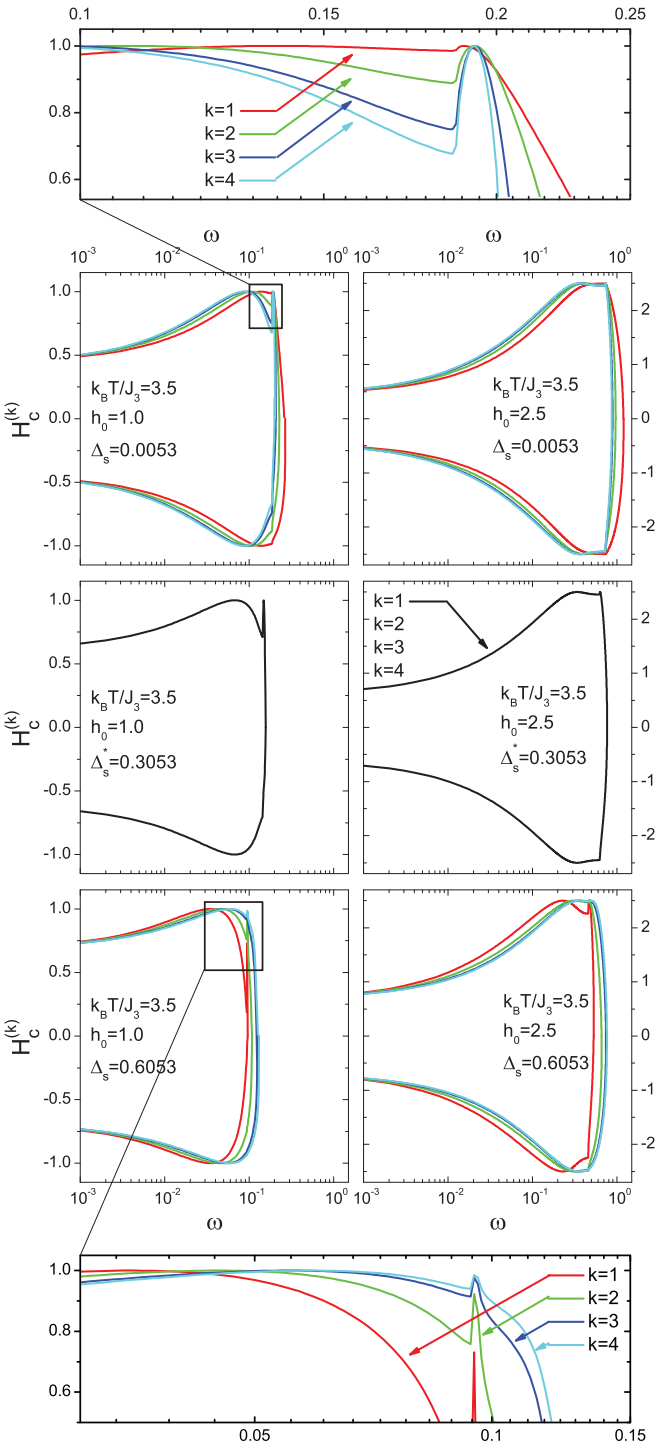

FIG. 2. (Color online) The frequency dispersion of a coercive field for the same selected system parameters of the film depicted in Fig. 1. The sequence of dispersions is reversed in two different regimes of modified exchange interaction.

to the phase lag. After ω_M, the hysteresis is still in a purely symmetric region with reversed shape for a while. In the $\Delta_s < \Delta_s^*$ regime, ω_M shifts to lower values with increasing layer index k (it means we are penetrating from the surface to the center) due to the locally stronger magnetic interaction. A_k also increases (especially at low ω) with increasing layer index k

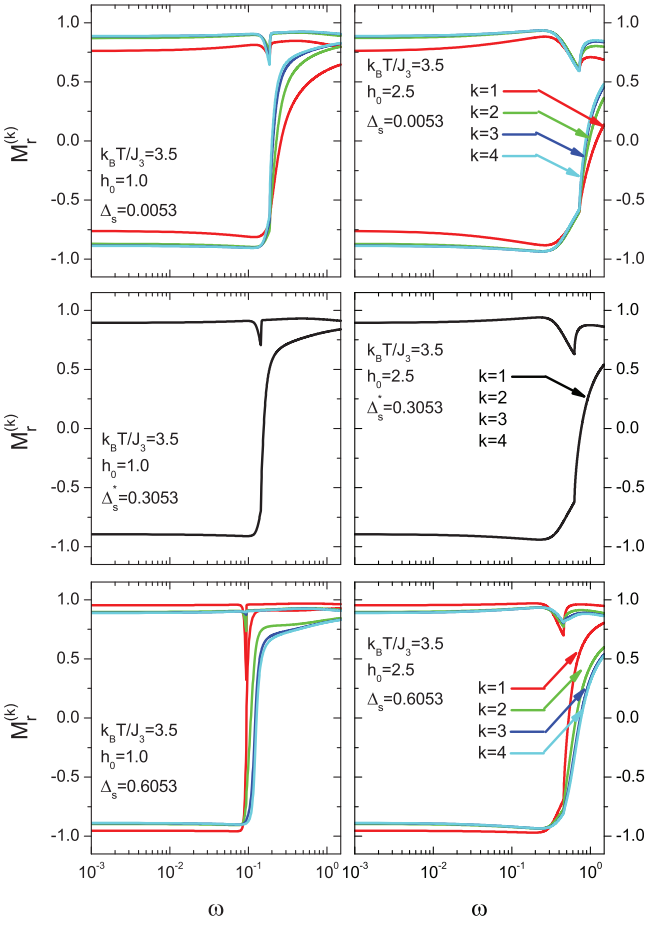

FIG. 3. (Color online) The frequency dispersion of remanent magnetization for the same selected system parameters of the film depicted in Fig. 1. The sequence of dispersions is reversed in two different regimes of modified exchange interaction.

for fixed ω in the same regime of Δ_s. The opposite of all these arguments can also be imagined for the $\Delta_s > \Delta_s^*$ regime. One can easily observe the intersection of layers via changing the Δ_s parameter at ω_M.

One can easily follow from Figs. 2 and 3, respectively, that the the coercivity $H_c^{(k)}$ is relatively large for a larger field amplitude h_0. The effect of a larger field amplitude h_0 on remanence $M_r^{(k)}$ can be seen also in the asymmetric region. A_k increases with increasing h_0, and this increment is independent of the other system parameters. This is since the magnetic energy due to the energy supplied by the external field in a cycle automatically becomes higher for higher amplitude values. This higher energy provides more magnetic force, which increases the ability of the spins to follow the external field sweep. Consequently, the corresponding frequency for the maximal peak (ω_M) in a symmetric region and the value of Δ_s shifts to higher frequencies. It is clear that the phase lag between the magnetization time series and external field signal is smaller for the higher amplitude.

The hysteresis loop collection of each layer for the selected system parameters together with three appropriate frequency values are presented in Fig. 4. In the low-frequency limit, the magnetization can be more saturated, and this shows itself as dominant magnetization processes in the different regions of the hysteresis (i.e., reversible boundary displacements, irreversible boundary displacements, and magnetization rotation). The figure shows that the hysteretic response of each layer clearly has the same characteristics at the critical value of the modified exchange Δ_s^* independently from the other parameters. Hierarchically changing the order of the hysteresis loop for various values of amplitudes and/or frequency also can be seen in Fig. 4 by following the group of three columns including the related regimes of Δ_s ($\Delta_s < \Delta_s^*$, $\Delta_s \equiv \Delta_s^*$ and $\Delta_s > \Delta_s^*$). One can observe the symmetry process in this order changing (corresponding to following the ability of the spin to make an external field sweep) by comparing the representative amplitudes between each other. For a Δ_s^* value and representative $h_0 = 2.5$, the hysteresis loop has a saturated s shape and tends to enhance its size with increasing ω at a low frequency region, e.g., $\omega < 0.3$. However, on further increasing ω, the loop gets its maximum area and later reduces to an oval shape with its major axis parallel to the field axis. This is the result of the phase lag between the magnetization time series and the field signal. At very low ω, the field period is large, and the magnetic spins have sufficient time to follow the field signal so the phase lag between the magnetization time series and field signal is very small. The system is strong enough to follow the external perturbation at those limitations, hence the hysteresis loop looks like a slim s shape. However, on increasing ω, the field sweeps faster. But the relaxation time of the system is fixed, so spins still have less time to follow the field. The phase lag gets larger, and so does the HLA. While the frequency value is approaching the correspondence phase lag, the hysteresis gets its maximum size, which corresponds to the frequency ω_M. After that, if ω still increases in small amounts, the system cannot follow the field, and the spins do not align in the same direction with ean xternal oscillatory field in each moment of a full cycle. Finally, the hysteresis dramatically loses its symmetry at a certain ω_C value. For $h_0 = 1.0$, a rare hysteresis shape and symmetry loss with increasing frequency can be seen by following the aforementioned topological evolution at the fixed $\Delta_s > \Delta_s^*$. For instance, as seen at $\omega = 0.07$, an exotic left-handed s shape beyond the oval form temporally takes place between the corresponding maximal area frequency ω_M and the frequency value of symmetry loss ω_C where $\omega_C > \omega_M$. The general trend mainly can be also explained as follows: For low frequencies, the hysteresis loop is in the form of a saturated s shape and tends to enhance its size with increasing ω at the low-frequency region. At ω_M value, the loop gets its maximum area. With a further increase in frequency, hysteresis enters into the process of smooth directional veering, and it changes its shape to a left-handed s shape until the symmetry loss. Finally, the symmetry loss occurs at a characteristic frequency value ω_C, so the hysteresis has an asymmetric shape.

The process stated at the beginning of directional veering and symmetry loss (between ω_M and ω_C) deserves scrutiny in terms of magnetic domain nucleation. As seen in Figs. 1–3, symmetry loss shows itself as a gibbous-like eminentia in ω_C. This phenomenon is also magnified in Figs. 1 and 2 for better visibility. In particular, as seen in Fig. 3, both positive and negative remanence appears at low frequencies, but only positive values survive at high frequencies. This

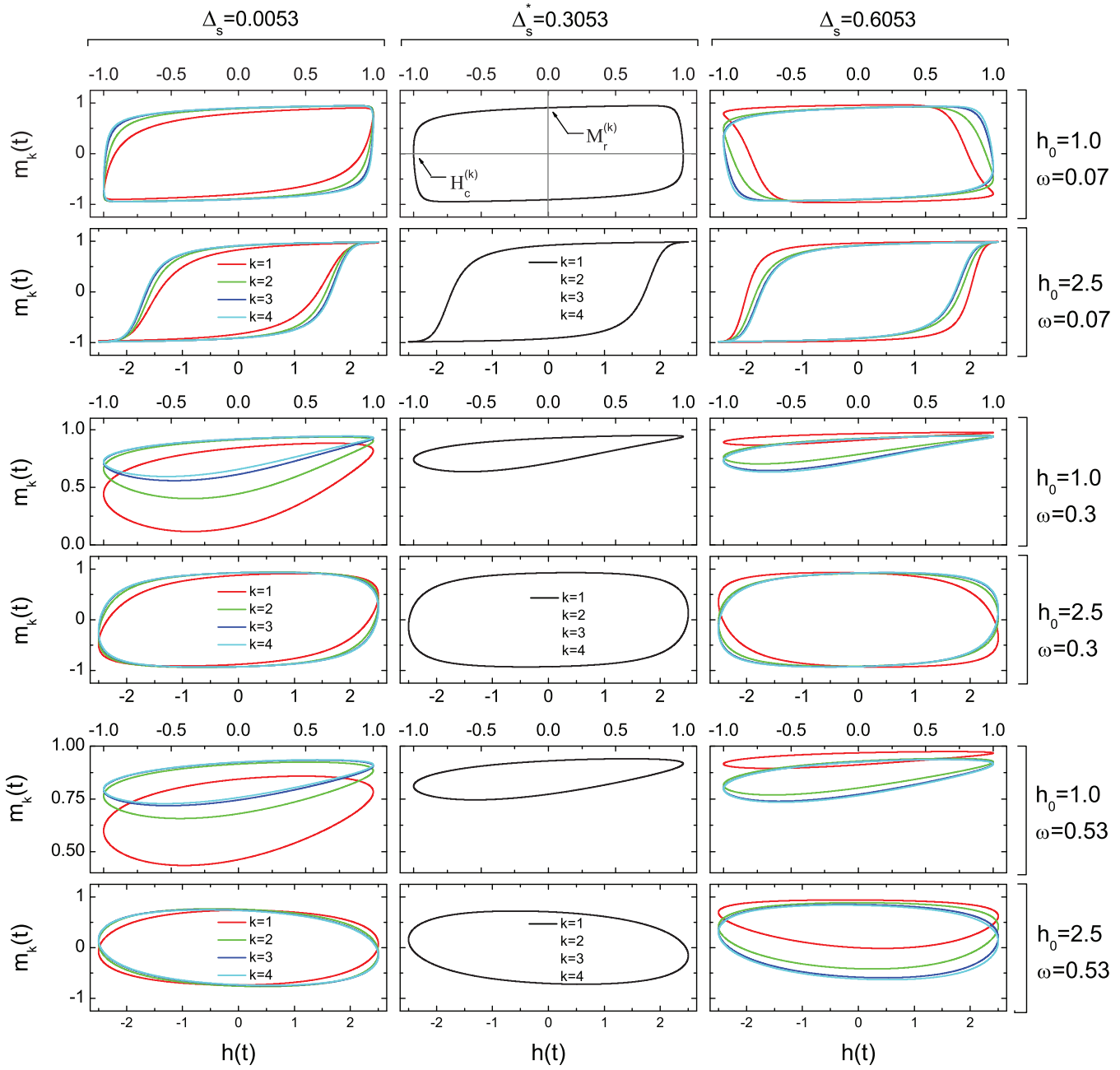

FIG. 4. (Color online) Well-selected hysteresis collection of each layer for the film with thickness $L = 7$. Modified exchange interaction Δ_s ranges from 0.0053 (first column) to 0.3053 (second column) and 0.6053 (third column) with varying frequency as $\omega = 0.07$, 0.3, and 0.53 for related amplitude representatives at $k_B T/J_3 = 3.5$. The reader can recognize the hierarchical evolution in the print gray-scale version by following the Supplemental Material given in in Ref. [19]. Here we note that the surface loop ($k = 1$) is more saturated in any case for $\Delta_s < \Delta_s^*$ value and the sequence of hysteresis is reversed in two different regimes of modified exchange interaction.

is also another indication of symmetry loss. The related eminentia shows itself more clearly on right arm of the mutual coercivity, and it is more and more distinct in surfaces for low amplitudes especially in the $\Delta_s > \Delta_s^*$ regime. We note that the encountered characteristics on this problem are members of the Type II.b family of frequency dispersion presented by Aktaş *et al.* [18,19]. As mentioned above, low amplitude relatively provides smaller magnetic energy to the system, and this weak energy could not provide enough magnetic force in causing the spins to follow the field. This means that the surfaces fall all over themselves to adopt to the asymmetric phase in the $\Delta_s > \Delta_s^*$ regime. So the surfaces have an extremely left-handed saturated s-shape hysteretic response within that period. It is also of special interest to consider the topological evolution of the hysteresis with varying ω to investigate how it relates with spin formation (magnetic domains) growth and/or nucleation mechanism. Two branches of the hysteresis almost lie on two perpendicular directions at ω_M. HLA has its maximum area, which is related to these two axes and their orientation. Therefore, the magnetic moments remain

a constant value in the half-time period of an external field at this frequency ω_M. At the fixed values of $\omega < \omega_M$ and $\omega > \omega_M$, respectively, corresponding hysteresis curves are topologically contraoriented, and completely different growth mechanisms are onset. The importance of this left-handed shape on the domain mechanism is that the domains currently continue to nucleate in a direction with a delay, while the magnetic field is increasing in the opposite direction in a half period of full cycle. This phenomenon should be considered especially in the fabrication process of thin films for magnetic recording purposes. A magnetization time series versus the external magnetic field, increasing the field frequency at first, obstructs the saturation of the ordinary magnetization due to the decreasing energy coming from the oscillating magnetic field in the half-time period, which facilitates the late-stage domain growth by tending to align the moments in its direction (i.e., the magnetization is no longer able to follow the oscillatory field). This enables a frequency increasing route to continuous dynamical phase transition due to the incomplete reversal of magnetic moments. The aforementioned directional-veering mechanism begins to lose its significance in the $\Delta_s < \Delta_s^*$ regime. When the Δ_s is lowered more and more, the dipole-dipole interaction-induced energy contribution becomes smaller. The strength of the energy contribution which comes from the dipole-dipole interaction corresponds to remaining in a dynamically symmetric phase of the system's own volition. Hence, the surfaces can stay in the symmetric phase in the smaller frequency until the frequency of the external field becomes greater than the intrinsic relaxation time of the system.

IV. CONCLUSION

The effect of modified exchange interaction on dynamical Ising-type thin film driven by an external oscillatory magnetic field is discussed by means of EFT based on standard DA. The time evolution of the system is presented by utilizing a Glauber-type stochastic process. The investigation is focused on frequency dispersion of HLA, coercivity, and the remanence of each layer.

In order to find the physical relation between domain growth and/or nucleation mechanism and symmetry loss, the topological evolution of the hysteresis with varying frequency is considered. Hence, some unpretentious improvements are developed in accordance with the explanations given in the literature [3–6].

The existence of a special transition point presented in Ref. [9] has been already confirmed by Tauscher and Pleimling via both Glauber and Metropolis dynamics [20]. Moreover, one can find to be of further interest the existence of a critical value of the surface exchange parameter at which all the layers seem to oscillate in phase. Based on the Monte Carlo results [20], we can say that the existence of a crossover in all hysteretic characteristics is not from the limitation of the method. This would hopefully provide some theoretical insight into the role of the surface layer and possibly some guidance for experimental studies on such systems.

In particular the short-time reversed shape of hysteresis in the frequency-induced evolution, which can be recognized only with such detailed examination as obtained from this work, is another issue worth considering. We hope that this study will shed light on further investigations of the dynamic nature of critical phenomena in pure crystalline ferromagnetic thin films and will be beneficial from both theoretical and experimental points of view.

ACKNOWLEDGMENTS

The numerical calculations in this paper were performed at TÜBİTAK ULAKBİM (Turkish agency), High Performance and Grid Computing Center (TRUBA Resources), and this study was completed at Dokuz Eylül University, Graduate School of Natural and Applied Sciences. B.O.A. would like to thank the Turkish Educational Foundation (TEV) for support.

[1] C. P. Steinmetz, Proc. of IEEE **72**, 197 (1984).
[2] J. S. Suen and J. L. Erskine, Phys. Rev. Lett. **78**, 3567 (1997).
[3] Q. Jiang, H. N. Yang, and G. C. Wang, Phys. Rev. B **52**, 14911 (1995).
[4] Y. L. He and G. C. Wang, Phys. Rev. Lett. **70**, 2336 (1993).
[5] J. S. Suen, M. H. Lee, G. Teeter, and J. L. Erskine, Phys. Rev. B **59**, 4249 (1999).
[6] Y. Laosiritaworn, Thin Solid Films **517**, 5189 (2009).
[7] H. Park and M. Pleimling, Phys. Rev. Lett. **109**, 175703 (2012).
[8] T. Osaka, T. Asahi, J. Kawaii, and T. Yokoshima, Electrochim. Acta **50**, 4576 (2005).
[9] B. O. Aktaş, Ü. Akıncı, and H. Polat, Thin Solid Films **562**, 680 (2014).
[10] R. J. Glauber, J. Math. Phys. **4**, 294 (1963).
[11] R. Honmura and T. Kaneyoshi, J. Phys. C: Solid State Phys. **12**, 3979 (1979).
[12] T. Kaneyoshi, Acta Phys. Pol. A **83**, 703 (1993).
[13] J. W. Tucker, J. Magn. Magn. Mater. **102**, 144 (1991).
[14] F. Zernike, Physica A **7**, 565 (1940).
[15] T. Balcerzak, J. Magn. Magn. Mater. **97**, 152 (1991).
[16] T. Kaneyoshi, R. Honmura, I. Tamura, and E. F. Sarmento, Phys. Rev. B **29**, 5121 (1984).
[17] T. Kaneyoshi, I. Tamura, and E. F. Sarmento, Phys. Rev. B **28**, 6491 (1983).
[18] B. O. Aktaş, Ü. Akıncı, and H. Polat, Physica B **407**, 4721 (2012).
[19] See Supplemental Material at http://link.aps.org/supplemental/10.1103/PhysRevE.90.012129 for the Type II.b class of frequency dispersion.
[20] K. Tauscher and M. Pleimling, Phys. Rev. E **89**, 022121 (2014).